One-Step Tailoring Surface Roughness and Surface Chemistry to Prepare Superhydrophobic Polyvinylidene Fluoride (PVDF) Membranes for Enhanced Membrane Distillation Performances

Weihua Qing [a], *Jianqiang Wang* [a, c], *Xiaohua Ma* [a,b], *Zhikan Yao* [a], *Yong Feng* [a], *Xiaonan Shi* [a], *Fu Liu* [c], *Peng Wang* [d], *Chuyang Y. Tang* [a,*]

a. Department of Civil Engineering, The University of Hong Kong, Pokfulam, Hong Kong 999077

b. Shanghai Key Laboratory of Multiphase Materials Chemical Engineering, School of Chemical Engineering, East China University of Science and Technology, 130 Meilong Road, Shanghai 200237, China

c. Key Laboratory of Marine Materials and Related Technologies, Ningbo Institute of Materials Technology and Engineering, Chinese Academy of Sciences, Ningbo, 315201, P. R. China.

d. Water Desalination and Reuse Center, Division of Biological and Environmental Sciences and Engineering, King Abdullah University of Science and Technology, Thuwal 23955-6900, Saudi Arabia

Abstract: Superhydrophobic polyvinylidene fluoride (PVDF) membrane is a promising material for membrane distillation. Existing approaches for preparing superhydrophobic PVDF membrane often involve separate manipulation of surface roughness and surface chemistry. Here we report a one-step approach to simultaneously manipulate both the surface roughness and surface chemistry of PVDF nanofibrous membranes for enhanced direct-contact membrane distillation (DCMD) performances. The manipulation was realized in a unique solvent-thermal treatment process, during which a treatment solution containing alcohols was involved. We demonstrate that by using different chain-length alcohols in the treatment solvent, surface roughness can be promoted by creating nanofin structures on the PVDF nanofibers using an alcohol which has

moderate affinity with PVDF. Meanwhile, surface chemistry can be tuned by adjusting the fraction distribution of crystal phases (nonpolar α phase and polar β phase) in the membrane using different alcohols. PVDF membranes with different surface wettabilities were used to evaluate the effects of surface roughness and surface energy on the DCMD performances. Combining both low surface energy and multi-scale surface roughness, pentanol-treated PVDF membrane achieved best anti-water property (water contact angle of 164.1° and sliding angle of 8.1°), and exhibited superior water flux and enhanced anti-wetting ability to low-surface-tension feed in the DCMD application.

Keywords: surface roughness, surface chemistry, membrane distillation, superhydrophobic membrane, polyvinylidene fluoride

1. Introduction

Water scarcity has been recognized as one of the largest humanity crisis [1–4], and increasing efforts have been devoted to convert seawater to fresh water [5–7]. Among many desalination techniques [8], membrane distillation (MD) has been gaining increasing attentions because it offers several attractive advantages, such as lower operating temperatures to distill water than conventional distillation, and lower pressure than reverse osmosis [9]. MD is thermally driven by partial vapor pressure difference across a porous hydrophobic membrane. In its most common configuration, direct-contact membrane distillation (DCMD), water from the hot feed side evaporate at the hydrophobic membrane surface before passing through the porous pores, and then condense at the other membrane side by the cooled permeate stream [10].

The ideal membrane for MD should have high porosity, chemical/thermal stability. Most importantly, it should be sufficiently hydrophobic to hold a stable liquid/vapor interfaces at the membrane pores to prevent wetting [11]. In this context, increasing efforts have been focused on the fabrication of superhydrophobic nanofibrous membranes by electrospinning technique for sustainable MD process [9]. Electrospinning is a promising technique to prepare porous membranes with high void volume fraction, controllable thickness and pore size [12], which will enable promoted water flux for MD. Moreover, membranes with superhydrophobicity often showed higher wetting resistance by minimizing contact area between the water droplet and the membrane surface [13,14].

Many polymers including polyvinylidene fluoride (PVDF), polyvinyl alcohol [15], polystyrene [16] have been electrospuned to fabricate nanofibrous membrane for MD. Among them, PVDF is the most popular material because of its outstanding features (high chemical resistance, thermal stability, and mechanical strength [17]). The pristine PVDF nanofibrous membrane often does not have superhydrophobicity, and a second post-treatment is often followed to further increase the anti-water property. Common post-treatment strategy include incorporating of nanoparticles first (e.g., TiO_2 [18], SiO_2 [19], carbon nanotube [20]), followed by surface coating of low surface energy chemicals (e.g., fluoroalkylsilane [21–24], polydimethylsiloxane [25,26], tetrafluoromethane [27]). Nevertheless, this strategy is based on incorporation of extrinsic additives, and often suffers from multi-step procedures and potential loss of the coating additives in long-term operation. In addition, most of low surface energy

topping are often expensive, non-biodegradable, and potentially harmful to environment and human health [28,29]. Therefore, development of simple and reliable approach to prepare superhydrophobic PVDF nanofibrous membrane is highly desirable.

In our recent study, we reported a novel solvent-thermal induced roughening (STIR) method to increase the surface roughness of polyvinylidene fluoride (PVDF) membranes [30]. The results revealed that roughness enhancement can be achieved by swelling of the membrane surface to create a soft shell/hard core structure under the combined action of solvent (water, hydrochloric acid and n-butanol) and heating, followed by a controllable surface roughening as a result of thermal-induced deformation of the soft shell (Figure 1a). The STIR method was capable of enhancing surface roughness for membranes with distinctly different pore structures, and opens up new possibilities to fabricate superhydrophobic membranes.

In the present study, we further demonstrate a one-step approach, based on the STIR, to simultaneously manipulate both the surface roughness and surface chemistry to prepare superhydrophobic PVDF membranes for enhanced MD performances. As illustrated in Figure 1b, a unique solvent-thermal treatment is applied to a pristine nanofibrous PVDF membrane, during which one certain kind of treatment solvent is added. We demonstrate that by using different kinds of alcohols in the treatment solvent, not only the surface roughness can be tailored through different affinities between the alcohols and the polymer (Figure 1a), but the surface chemistry of the membrane can also be tuned by manipulating the crystalline phase transformation of PVDF between polar β-phase (hydrophilic) and nonpolar α-phase (hydrophobic) (Figure 1c). By using

PVDF membranes with different surface energy and roughness, we further evaluate the effect of membrane surface energy and surface roughness on MD performances.

2. Materials and methods

2.1. Materials:

PVDF powder was obtained from Aldrich with average Mw of ~180000 Da. Hydrogen chloride (HCl, 37wt.%), Sodium chloride, N,N-Dimethylformamide (DMF), isopropanol, 1-butanol, 1-pentanol, 1-heptanol and 1-decanol were purchased from VWR Chemicals Ltd.. Sodium dodecyl sulfate (SDS) is a commonly used anionic surfactant and was received from Uni-Chem Inc.. Milli-Q water (Millipore) was used in this study.

2.2. Pristine PVDF nanofibrous membrane preparation

A polymer solution first was obtained by dissolving 5 g PVDF polymer beads in 15 g DMF at 60 ^{o}C under stirring overnight. A pristine PVDF nanofibrous membrane was then prepared using electrospinning technique with the following conditions: flow rate of polymer solution = 0.88 mL/h, applied voltage = 24 kV, spinneret to collector distance = 15 cm. A total solution volume of 15 mL was electrospuned. The resultant PVDF nanofibrous membrane was heated in a vacuum oven at 60 ^{o}C overnight to evaporate the residual solvent before further treatment.

2.3. One-step tailoring of surface roughness and surface chemistry

The simultaneous manipulation of both the surface roughness and surface chemistry of the membrane was realized by a modified STIR method [30]. Typically, a

treatment solution containing HCl (15 mL), Milli-Q water (15 mL), and a certain kind of alcohols (4.32 mL) was prepared in a Teflon-lined autoclave. One small piece of nanofibrous coupon (3cm × 3cm) was immersed in the solution before the autoclave was put inside an electric oven at 150 ^{o}C for 4 hours. Afterwards, the membrane coupon was taken out of the autoclave, and rinsed with ethanol in an ultrasonic cleaner for several times to remove any residual treatment solution. Finally, the membrane coupon was dried in the electric oven at 60 ^{o}C before further usage.

2.4. QCM analysis

The different affinities of alcohols with PVDF were measured using a Quartz Crystal Microbalance (QCM, Biolin Scientific, Sweden). A dilute PVDF solution (0.5 wt.%) was first obtained by dissolving the PVDF powder in DMF and stirring the mixture at 60 ^{o}C overnight. Then a PVDF thin film was fabricated by first applying 5 μL polymer solution on a gold-coated wafer and then allowing film solidification in the oven at 60 ^{o}C. After the PVDF-coated wafer was placed in the test cell of QCM, one certain type of alcohol was introduced into the cell at a flow rate of 80 μL/min. The absorption quantity of alcohols on the PVDF film was characterized by the frequency change through the Sauerbrey equation.

2.5. Characterization

SEM images of the membranes were characterized by a Field Emission Gun Scanning Electron Microscope (LEO1530 FEG SEM, UK). FTIR-ATR analysis was conducted through a Nicolet 8700 in the wavenumber range of 4000-500 cm^{-1}. X-ray photoelectron spectroscopy (XPS) spectra of the membrane surfaces were analyzed by

ESCALAB250 from Thermo Fisher Scientific, with an X-ray source of monochromic Al Kα 150W. X-ray diffraction of the samples were performed on a Bruker D8 advanced X-ray diffractometer (Karlsruhe, Germany) equipped with a Cu $K\alpha_{1,2}$ X-ray irradiation source at room temperature. The 2θ scanning range was between 10–80°, and the scanning rate was 0.03°/s. Sliding angles were measured by a goniometer (HWHR Instruments, China). Static contact angles (SCA) were measured by Attention Theta (Biolin Scientific, Sweden). Each water droplet (~6 μL) was applied to the membrane surface, and allowed a stabilizing time of approximate 10 s. Six measurements were performed for each membrane sample, and the average values were reported.

2.6. Direct-contact membrane distillation experiments

The DCMD experiments were performed in a custom-made setup as shown in our previous study [30]. The effective area for MD was 9 cm^2 (1.5 cm × 6 cm), and all the tubes were wrapped with insulating tubes to minimize heat loss. In a typical DCMD experiment, feed water of 1.5 L NaCl solution (3.5 wt.%) was circulated in the feed side of the cell at 60 ± 0.5 °C with a flow rate of 0.48 L/min, and permeate stream of Milli-Q water was circulated (counter-current direction with the feed stream) at the permeate side at 20 ± 0.5 °C with a slightly slower flow rate of 0.44 L/min. The permeate container was placed on an electronic balance to obtain the weight increase for flux calculation, and a conductivity probe was submerged in the container to measure the permeate conductivity.

To investigate the anti-wetting performances towards low surface energy feed of the membranes, after an initial 2 hours of stabilization period, 0.05 mM surfactant SDS

was added into the feed solution every 2 hours to progressively decrease the feed surface tension. Other experimental conditions were similar with the typical DCMD tests.

3. Result and discussion

3.1. Surface morphology

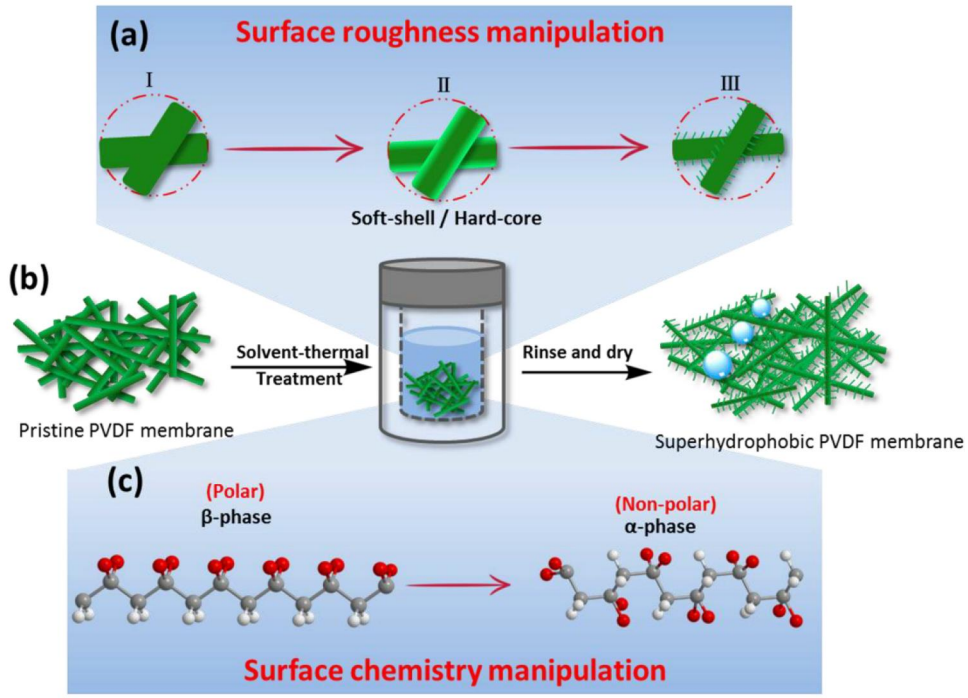

Figure 1. Schematic illustration of one step manipulation of surface roughness and chemistry of PVDF membrane: (a) nanofin structures formation on the pristine nanofiber, leading to a promoted surface roughness; (b) treatment procedures for superhydrophobic modification; (c) Transition of polar β phase to nonpolar α phase, leading to a promoted hydrophobicity of the material.

In a typical process, a pristine nanofibrous PVDF membrane was first prepared using electrospinning technique [31]. A solvent-thermal treatment solution containing HCl, Milli-Q water and one certain kind of alcohol was prepared in a Telfon-lined autoclave. Then the membrane was immersed in the treatment solution and

hydrothermally treated at 150 ^{o}C for 4 hours to get the treated membrane. The variation of surface morphology and surface chemistry of the membranes as well as their wetting properties were characterized.

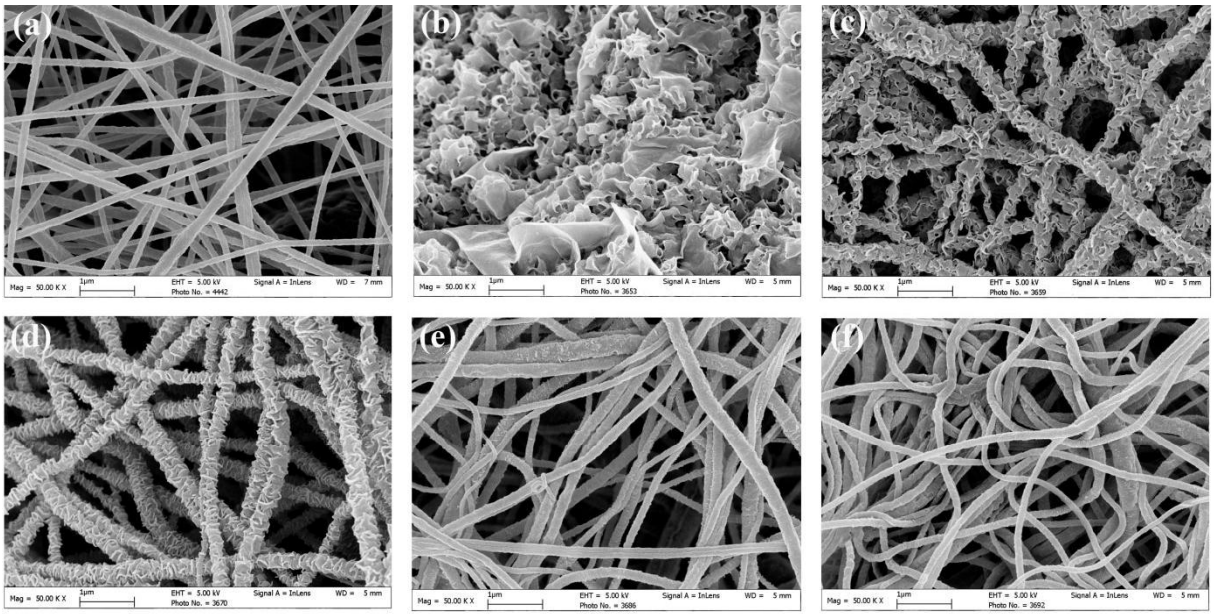

Figure 2. Effects of alcohol types on the morphology of the PVDF nanofibrous membranes: (a) pristine membrane; Treated membranes using (b) isopropanol, (c) 1-butanol, (d) 1-pentanol, (e) 1-heptanol and (f) 1-decanol. Solvent-thermal treatment conditions: HCl:water:alcohol=15mL:15mL:4.32mL, 150 ^{o}C, 4 hours.

To unravel the role of alcohol types on the surface morphology of the PVDF nanofibrous membrane in the STIR treatment, we modified the pristine PVDF membrane with alcohols of different chain lengths, $C_nH_{2n+2}O$ (n=3, 4, 5, 7, 10). Figure 2 shows that the morphologies of STIR-treated membrane were remarkably different depending on the chain length. The pristine PVDF nanofiber had a three-dimensional porous structure and the surface of the nanofiber was very smooth (Figure 2a). However, when isopropanol (n=3) was used in the treatment solution, nanofin structures was formed to result in a very rough surface. Nevertheless, the backbone and the porous structure of the resultant membrane were completely destroyed (Figure 2b). With

increasing the chain length of alcohols from 1-butanol (n=4) to 1-pentanol (n=5), the three-dimensional network structure of the membrane were maintained, with nanofin structures densely-packed along the nanofiber (Figure 2c-d). These observations were further confirmed by average roughness measurement using atomic force microscopy (see AFM micrographs in Fig. S1 in supporting information and the summarized results in Table 3). The roughness enhancement by nanofins coverage could be attributed to the combined solvent and thermal treatment. According to our previous study [30], this treatment process partially swells the pristine PVDF nanofiber, leading to a swelled soft-shell surrounding a hard-core (non-swelled part) and consequently the deformation of the shell under the mismatched internal stresses between the shell and the core. Further increasing the alcohol chain length (n=7, 10), the secondary nanostructure on the nanofiber gradually disappeared (Figure 2e-f).

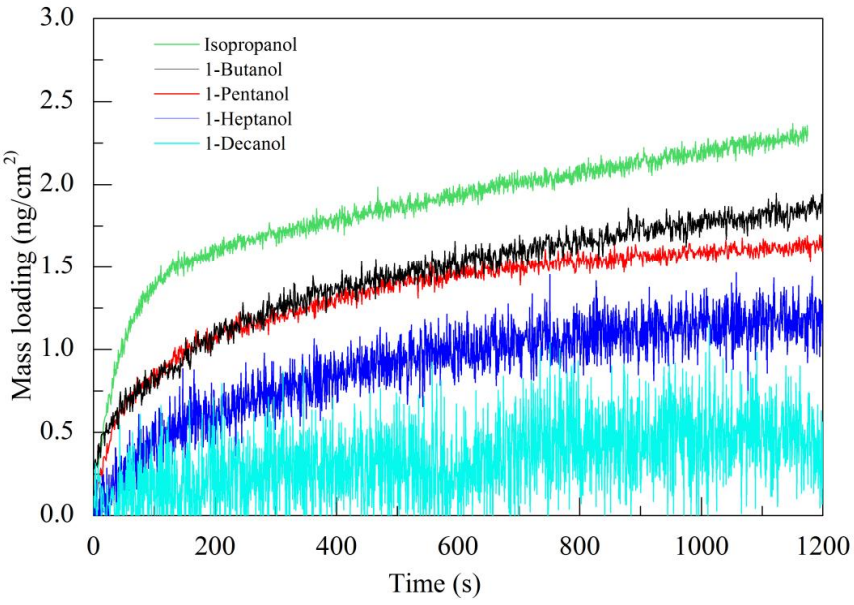

Figure 3. The mass loading of alcohols on the PVDF membranes in QCM, showing different affinity between alcohols with PVDF.

Table 1 Difference of solubility parameters between PVDF and alcohols

	Carbon numbers	δ_T [a] ($Mpa^{1/2}$)	$\Delta\ \delta_{T,P-S}$
PVDF	-	25.2	-
Isopropanol	3	23.6	1.6
1-Butanol	4	23.2	2.0
1-Pentanol	5	21.9	3.3
1-Heptanol	7	20.5	4.7
1-Decanol	10	19.4	5.8

a. Temperature 25 ^{o}C; Ref.[32–34] for PVDF and Ref.[35] for alcohols.

To better understand the observed different effects of alcohols on the morphology of treated PVDF membrane, we further measured the affinity between alcohols and PVDF using a quartz crystal microbalance (QCM). Clearly, the mass of alcohols absorbed on the PVDF membrane decreased with increasing the alcohol chain lengths (Figure 3), indicating that PVDF has lower affinity to longer-chain alcohols. The compatibility between the PVDF and alcohols can also be evaluated by calculating the difference of their solubility parameters [36]:

$$\Delta\delta_{T,P-S} = \delta_{T,P} - \delta_{T,S} \qquad (1)$$

where $\delta_{T,P}$ and $\delta_{T,S}$ are the solubility parameters of PVDF and alcohols, respectively. As shown in Table 1, the difference $\Delta\delta_{T,P-S}$ is larger when increasing the carbon chain length of alcohols, further confirming poorer compatibility between PVDF and the longer-chain alcohols.

Together with the membrane morphology variation, these observations imply that a moderate affinity between the alcohol and PVDF is essential to enable partial swelling of the nanofiber, which promotes formation of a uniformly nanofin-covered nanofibrous

membrane (n=4, 5). Severe swelling (i.e., excessive absorption of alcohol and lower $\Delta\delta_{T,P\text{-}S}$ value) will destroy the nanofiber backbone as a result of entire deformation of the fiber in the treatment process (n=3). In contrast, insufficient absorption of alcohol fails to partially swell the nanofiber and thus inhibits the creation of the soft-shell/hard core structure (see Figure 1a). Consequently, the formation of nanofins cannot be realized (n=7, 10).

3.2.Surface chemistry

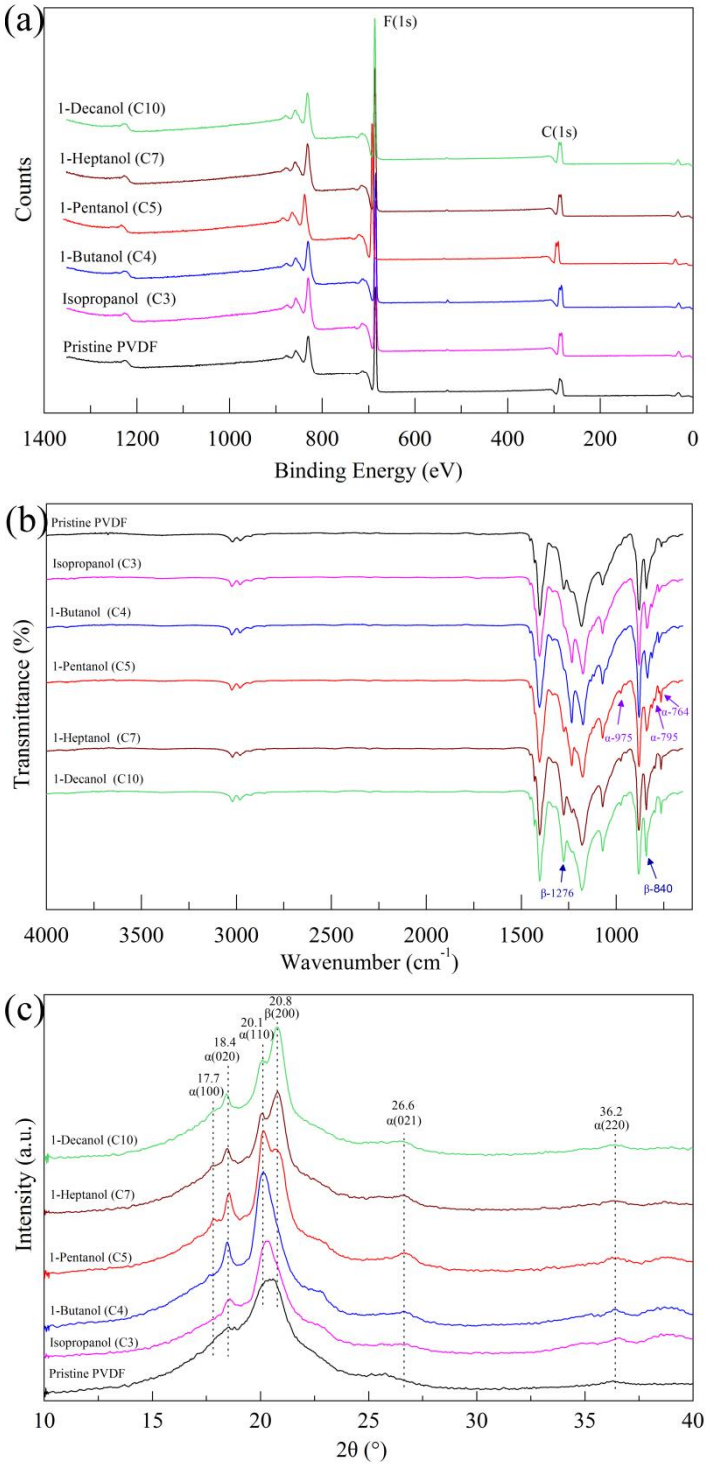

Figure 4. Surface chemistry characterizations of pristine PVDF membrane and different-alcohol-treated membranes: (a) XPS survey spectra, (b) FTIR spectra, and (c) XRD spectra.

Manipulation of surface chemistry is another key for preparation of superhydrophobic surfaces [37]. Figure 4a presents the X-ray photoelectron

spectroscopy (XPS) survey spectra of PVDF membranes before and after STIR treatment. It can be seen that the spectra were similar and only the element of carbon and fluorine were detected for all the membrane samples. The carbon / fluorine atomic ratios of the treated membrane were also found to be ~ 1.0, which is consistent with the chemical formula of pristine PVDF ($[C_2H_2F_2]_n$). This observation is in good agreement with our previous study [30], suggesting that no chemical grafting occurred during the treatment process.

FTIR analysis of the membranes is shown in Figure 4b. The peaks at 764, 795, 975 cm^{-1} were assigned to nonpolar α phase crystal in PVDF (α-PVDF), and the peaks at 840, 1276 cm^{-1} were assigned to polar β phase crystal in PVDF (β-PVDF) [38–40]. Interestingly, though no additional groups were observed on the spectra of the treated membrane when compared to the pristine one, the amount distribution of crystal forms in PVDF was apparently affected by using different alcohols. Motivated by this observation, we further quantified the α and β phase fractions by using the peaks at 764 cm^{-1} and 840 cm^{-1} according to the following equation [41,42]:

$$F(\alpha) = \frac{A_\alpha}{(K_\alpha / K_\beta)A_\beta + A_\alpha} \qquad (2)$$

where $F(\alpha)$ represents the fraction of α-PVDF. A_α and A_β are the absorbencies at 764 and 840 cm−1, and can be calculated by applying A=2-Lg%T (where T is the transmittance). K_α (6.1×10^4 cm^2/mol) and K_β (7.7×10^4 cm^2/mol) represent the absorption coefficients at the respective wave number.

The results are summarized in Table 2. The pristine PVDF membrane had a α

phase fraction of 21%. The α-PVDF fraction first increased to 33% when increasing the chain length of the alcohol to 5 (1-pentanol). Further increase the carbon number of the alcohol led to a gradual decrease to 27% (1-Decanol) of the nonpolar α phase fraction in the membrane. This observation was further confirmed by XRD analysis (Figure 4c). The peaks at 17.7°, 18.4°, 20.1°, 26.6° and 36.2° were assigned to (100), (020), (110), (021) and (220) reflections of the crystallographic planes of α-PVDF [42–44]. The intensities of these peaks reached maximum for the membrane treated by 1-pentanol.

Table 2 α phase fractions in the pristine and treated PVDF membranes

	Carbon number	Transmittance		Absorbance		α fraction %
		β	α	β	α	
Pristine	-	67.1	91.8	0.173	0.037	21
Isopropanol	3	69.5	91.1	0.158	0.040	24
1-Butanol	4	64.2	89.2	0.192	0.050	25
1-Pentanol	5	69.7	86.7	0.157	0.062	33
1-Heptanol	7	62.7	86.6	0.203	0.062	28
1-Decanol	10	61.1	86.5	0.214	0.063	27

3.3.Wettability

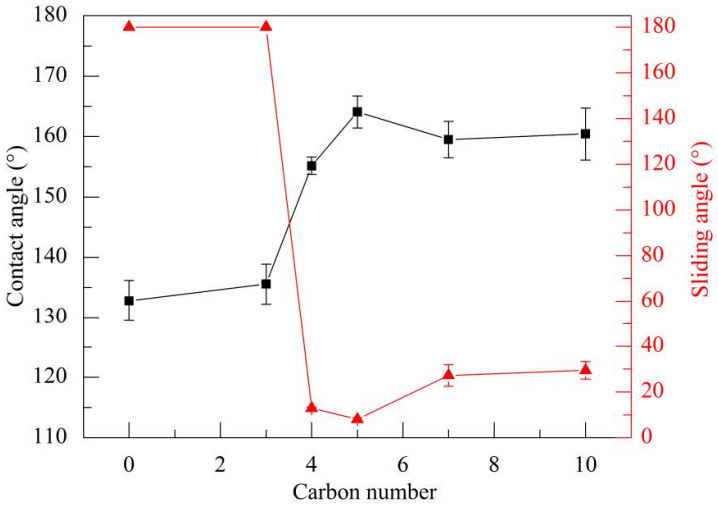

Figure 5. Effects of alcohol types on the water contact angles and sliding angles of pristine and treated PVDF membranes

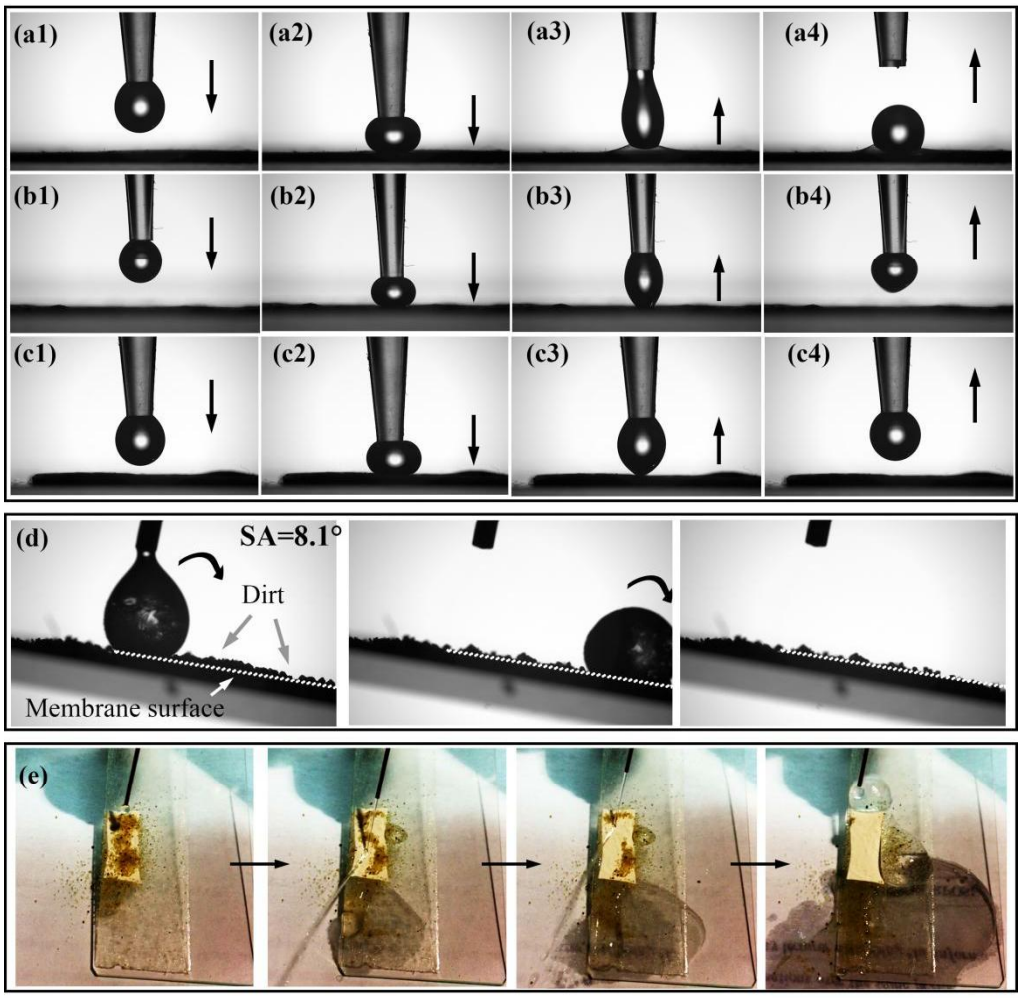

Figure 6. Wettability characterizations for different PVDF membranes: Photos of dynamic measurements of water contacting the (a) pristine membrane, (b) decanol-treated membrane, and (c) pentanol-treated membrane; (d) sliding angle measurement of the pentanol-treated membrane, showing one water droplet rolling off the membrane surface and carrying dirt with it. (e) Photos showing a stream of water bouncing off the pentanol-treated membrane surface and removing the dirt.

Figure 5 shows the effects of alcohol types on the water contact angle and sliding angle. The pristine PVDF membrane had a water contact angle of 132.8° and a sliding angle of 180° (The water droplet pinned on the surface when the membrane was turned upside down). When treated by STIR method using different alcohols, the membranes showed an increased water contact angles. A superhydrophobic property (contact angle higher than 150°) was obtained for alcohols of chain length over 4. The improved

anti-water performance of the membranes can be attributed to the roughness enhancement as shown in Figure 2b-f. Moreover, the water sliding angles of the membranes first decreases to 8.1° when increasing the chain length of the alcohol to 5 (1-pentanol), followed by a gradual increase of sliding angle to 29.5° when further increase the carbon number of the alcohol to 10 (1-Decanol). The sliding angle behaviors were in good agreement with the fraction variation of nonpolar α-PVDF in the membranes when increasing the chain length of the alcohols (Table 2). The observation agrees with the conclusions by many studies that larger fraction of nonpolar α-PVDF reduces the surface energy of the material [40–42], thus leading to an improved water mobility of the membrane.

The membrane treated by 1-pentanol exhibited the best anti-wetting ability with highest water contact angle of 164.1° and a sliding angle of 8.1°, which can be attributed to a combination of high surface roughness (Figure 2d) and low surface energy (i.e., high nonpolar α-PVDF fraction). Meanwhile, though decanol-treated membrane did not exhibit high surface roughness (Figure 2f), it still achieved superhydrophobicity due to promoted α-PVDF fraction (corresponds to low surface energy). Figure 6a-c shows the water repelling properties of the pristine, decanol-treated, and pentanol-treated membranes by examining the dynamic wetting behavior of water on the membranes. A high-speed camera was used to record the contacting process of a water droplet on the membrane. The droplet was forced to sufficiently contact the membrane surface with an obvious deformation, and then it was lifted up. Remarkably, the water droplet was dramatically elongated before it deposited on the pristine

membrane during the process (Figure 6a), indicating a strong adhesion of the water droplet with the pristine membrane. The sticky property implies that the wetting behavior of a water droplet on pristine PVDF membrane may fall in the Wenzel regime. Under this regime, the liquid drop will enter and fill the interstices among the nanofibers, resulting in high adhesion towards the surface [45]. In contrast, though the droplet also elongated on the decanol-treated membrane (Figure 6b) when lifting up, it was eventually stick away by the syringe needle. The pentanol-treated membrane showed the weakest interaction with the water droplet because the droplet was only slightly stretched before it was finally stick away (Figure 6c). These two observations indicate the water wetting behavior gradually switched from the Wenzel state to the Cassie-Baxter state after the membrane was treated by 1-decanol and 1-pentanol. The water droplet cannot entering into the air pockets between the nanofibers (illustrated in Figure 7c), leading to a significantly reduced adhesion of the droplet with the membrane [46]. The excellent non-sticky property of the pentanol-treated membrane was further demonstrated in Figure 6d-e, where small water droplet could easily roll off the membrane surface and carry dirt away with it.

3.4. DCMD applications

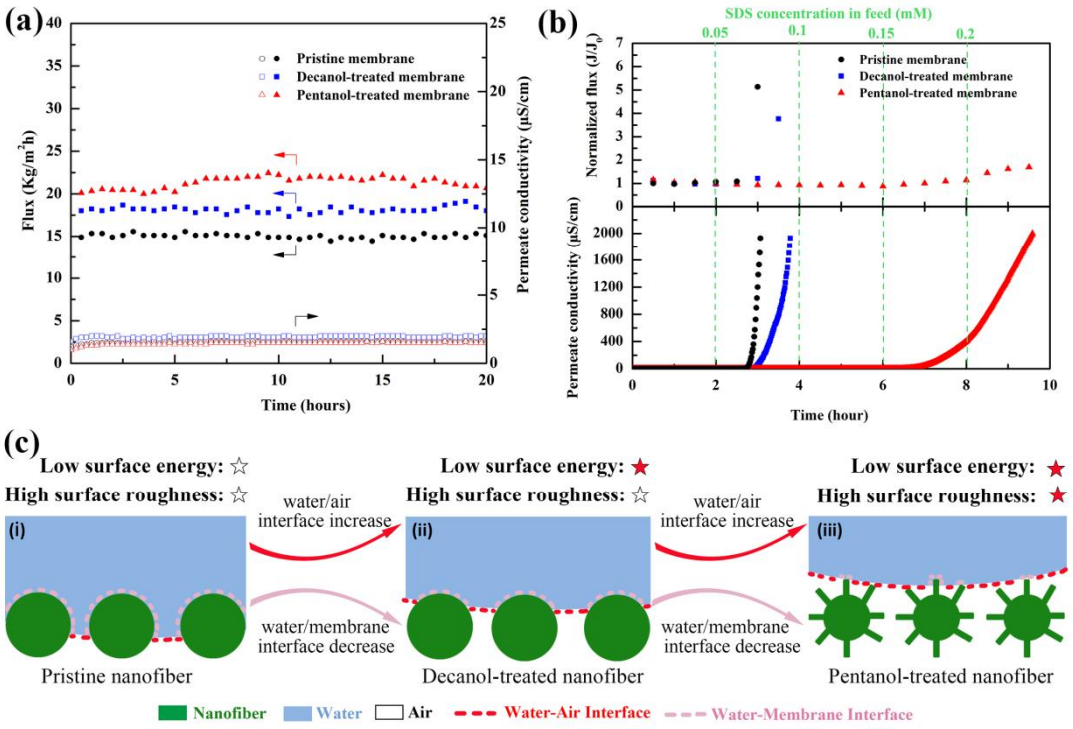

Figure. 7 DCMD applications with the pristine, decanol-treated, and pentanol-treated PVDF membranes: (a), Permeate flux and permeate conductivity with feed solution of 3.5 wt.% NaCl at 60 ^{o}C and permeate stream of water at 20 ^{o}C. (b), Anti-wetting abilities of different PVDF membranes with progressive addition of SDS in 3.5 wt.% NaCl feed solution. (c), Schematic illustration of possible wetting behaviors of a water droplet on pristine, decanol-treated, or pentanol-treated membranes.

Table 3 Properties and wettability of pristine, decanol-treated, and pentanol-treated membranes

	Pristine membrane [a]	Decanol-treated membrane	Pentanol-treated membrane
Mean fiber diameter (nm)	202±66	213±55	330±63
Fiber average roughness (nm) [b]	3	4	15
Porosity (%)	89±1.3	86±0.2	83±1.6
BET surface area (m^2/g)	7.3	7.7	14.6
Max pore size (nm)	1054±119	971±20	674±75
Mean pore size (nm)	909±5	592±8	468±6
Thickness (mm)	0.24±0.04	0.23±0.05	0.27±0.04
Contact angle [c] (deg.)	132.8±3.4	160.4±4.3	164.1±2.4
SDS contact angle [d] (deg.)	108.7±7.8	142.3±3.7	159.9±1.8
Sliding angle (deg.)	180	29.5±3.8	8.1±0.7
LEP (kPa)	83±3	131±5	182±7

[a] Some properties of pristine membrane were adapted from our previous report [30].

[b] Detailed AFM characterization of pristine and treated membranes can be found in supporting information (Figure S1).

[c] Contact angle measured by DI water (surface tension = 72.6 mN/m).

[d] Contact angle measured by 3.5 wt % NaCl solution containing 0.05 mM SDS (surface tension

= 63.6 mN/m)

As shown in the previous section that pristine, decanol-treated and pentanol-treated PVDF membranes exhibited different surface wettabilities due to their different surface energy/surface roughness combinations. To evaluate the effect of surface energy and roughness on desalination performances, the three types of membranes were used in DCMD experiments with a synthetic seawater (3.5 wt.% NaCl) as feed solution under a temperature of 60 ^{o}C, and the permeate side was set at 20 ^{o}C. As shown in Figure 7a, all the three membranes showed stable water fluxes and produced high quality water with conductivities below 5 μS/cm. When compared to the pristine membrane, the average water flux was promoted from ~15 to ~17 Kg/m^{2}h by using the decanol-treated membrane, while the pentanol-treated membrane exhibited a highest average water flux of ~21 Kg/m^{2}h. Considering the fact that the porosity and mean pore size of the decanol-treated and pentanol-treated membrane were smaller than that of the pristine one (see Table 3), we attribute the superior water flux to higher water/air interfacial area when wetting mechanism switched from Wenzel model to Cassie-Baxter model. As illustrated in Figure 7c, since the wetting behavior of pristine membrane most likely fall in Wenzel regime, the water can penetrate into the voids between the nanofibers (resulting in a smallest water/air interface) [47]. In contrast, the water wetting behavior of decanol-treated membrane gradually switched from the Wenzel state to the Cassie-Baxter because lower surface energy of the membrane prevents water penetration into the nanofibers, leading to an increase of the water/air interface [48]. The water/air interface is expected to be further promoted by increasing the surface

roughness (pentanol-treated membrane), because water can be supported on the secondary nanofins of the membrane. Promoting water/air interfaces enable larger effective liquid evaporation areas and suffer smaller conductive heat loss to the surroundings [49], thus resulting in enhanced permeation flux in DCMD experiment.

The anti-wetting abilities of the membranes toward low surface tension feed were also investigated in DCMD. After an initial 2 hours of stabilization period, 0.05 mM surfactant SDS was added to the feed solution every 2 h to progressively decrease the feed surface tension. As shown in Figure 7b, the pristine PVDF membrane showed a sudden increase in both the flux and permeate conductivity shortly after 0.05 mM SDS addition, indicating a poor anti-wetting ability to low surface tension feed. The decanol-treated membrane was also wetted by 0.05 mM SDS dosage, but maintained a slightly longer time operation. The pentanol-treated membrane exhibited stable flux and permeate conductivity for SDS concentrations up to 0.1 mM and was wetted only after 0.15 mM SDS dosage. The enhanced wetting resistance of the pentanol-treated membrane is also reflected by its higher SDS contact angle as shown in Table 3. These results demonstrated the importance of combining both low surface energy and multi-scale surface roughness on a superhydrophobic membrane for enhanced DCMD performances. Long term performance of the pristine and STIR-treated membrane in DCMD can be found in our previous report [30].

4. Conclusions

In summary, we have shown a one-step approach to manipulate both the surface roughness and surface chemistry to prepare superhydrophobic PVDF nanofibrous membranes for enhanced DCMD performances. The surface roughness can be tailored by creating nanofin structures on the PVDF nanofibers using an alcohol which is moderately compatible with the PVDF material. The moderate affinity between PVDF and alcohol is essential for controllable nanofins formation because this enable partial swelling of the PVDF nanofiber to form a unique soft-shell/hard-core transitional structure, followed by a controllable deformation of the soft shell (resulting from mismatched internal stresses between the shell and the core). Meanwhile, the surface chemistry can be tuned by adjusting the fraction distribution of crystal phases (mainly nonpolar α phase and polar β phase) in the membrane using different alcohols. We showed that the use of 1-pentanol in the STIR process promote both the surface roughness and the nonpolar α-PVDF fraction of the membrane, leading to a superior anti-wetting ability of the membrane with a water contact angle of 164.1° and a sliding angle of 8.1°. Benefited from the combination of low surface energy and multi-scale roughness, the pentanol-treated membrane exhibited superior desalination flux, which can be possibly attributed to its higher water/air interfacial area. Moreover, the pentanol-treated membrane also showed best anti-wetting ability towards low surface tension in DCMD application.

Acknowledgements

We thank the financial support from the Office of Sponsored Research, King

Abdullah University of Science and Technology (No. OSR-2017-CPF-3320), and partial funding support by Joint Research Scheme (National Natural Science Foundation of China and Research Grants Council of Hong Kong) (N_HKU706/16).

References:

[1] M.M. Mekonnen, A.Y. Hoekstra, Four billion people facing severe water scarcity, Sci. Adv. 2 (2016) e1500323–e1500323. doi:10.1126/sciadv.1500323.

[2] R.F. Service, Desalination freshens up., Science. 313 (2006) 1088–90. doi:10.1126/science.313.5790.1088.

[3] X.-H. Ma, H. Guo, Z. Yang, Z.-K. Yao, W.-H. Qing, Y.-L. Chen, Z.-L. Xu, C.Y. Tang, Carbon nanotubes enhance permeability of ultrathin polyamide rejection layers, J. Memb. Sci. 570–571 (2019) 139–145. doi:https://doi.org/10.1016/j.memsci.2018.10.055.

[4] S. Shao, W. Fu, X. Li, D. Shi, Y. Jiang, J. Li, T. Gong, X. Li, Membrane fouling by the aggregations formed from oppositely charged organic foulants, Water Res. 159 (2019) 95–101. doi:https://doi.org/10.1016/j.watres.2019.05.004.

[5] P.D. Dongare, A. Alabastri, S. Pedersen, K.R. Zodrow, N.J. Hogan, O. Neumann, J. Wu, T. Wang, A. Deshmukh, M. Elimelech, Q. Li, P. Nordlander, N.J. Halas, Nanophotonics-enabled solar membrane distillation for off-grid water purification., Proc. Natl. Acad. Sci. U. S. A. 114 (2017) 6936–6941. doi:10.1073/pnas.1701835114.

[6] M. Elimelech, W.A. Phillip, The future of seawater desalination: energy, technology, and the environment., Science. 333 (2011) 712–7. doi:10.1126/science.1200488.

[7] Z. Yao, H. Guo, Z. Yang, W. Qing, C.Y. Tang, Preparation of nanocavity-contained thin film composite nanofiltration membranes with enhanced permeability and divalent to monovalent ion selectivity, Desalination. 445 (2018) 115–122. doi:https://doi.org/10.1016/j.desal.2018.07.023.

[8] A. V. Dudchenko, C. Chen, A. Cardenas, J. Rolf, D. Jassby, Frequency-dependent stability of CNT Joule heaters in ionizable media and desalination processes, Nat. Nanotechnol. 12 (2017) 557–563. doi:10.1038/nnano.2017.102.

[9] P. Wang, T.-S. Chung, Recent advances in membrane distillation processes: Membrane development, configuration design and application exploring, J. Memb. Sci. 474 (2015) 39–56. doi:10.1016/J.MEMSCI.2014.09.016.

[10] Abdullah Alkhudhiri, Naif Darwish, Nidal Hilal, Membrane distillation: A

comprehensive review, Desalination. 287 (2012) 2–18. doi:10.1016/J.DESAL.2011.08.027.

[11] A. Deshmukh, C. Boo, V. Karanikola, S. Lin, A.P. Straub, T. Tong, D.M. Warsinger, M. Elimelech, Membrane distillation at the water-energy nexus: limits, opportunities, and challenges, Energy Environ. Sci. (2018). doi:10.1039/C8EE00291F.

[12] W. Qing, X. Shi, Y. Deng, W. Zhang, J. Wang, C.Y. Tang, Robust superhydrophobic-superoleophilic polytetrafluoroethylene nanofibrous membrane for oil/water separation, J. Memb. Sci. 540 (2017). doi:10.1016/j.memsci.2017.06.060.

[13] A.K. An, J. Guo, E.-J. Lee, S. Jeong, Y. Zhao, Z. Wang, T. Leiknes, PDMS/PVDF hybrid electrospun membrane with superhydrophobic property and drop impact dynamics for dyeing wastewater treatment using membrane distillation, J. Memb. Sci. 525 (2017) 57–67. doi:10.1016/j.memsci.2016.10.028.

[14] Y. Liao, R. Wang, A.G. Fane, Fabrication of Bioinspired Composite Nanofiber Membranes with Robust Superhydrophobicity for Direct Contact Membrane Distillation, Environ. Sci. Technol. 48 (2014) 6335–6341. doi:10.1021/es405795s.

[15] Y.-X. Huang, Z. Wang, D. Hou, S. Lin, Coaxially electrospun super-amphiphobic silica-based membrane for anti-surfactant-wetting membrane distillation, J. Memb. Sci. 531 (2017) 122–128. doi:10.1016/J.MEMSCI.2017.02.044.

[16] X. Li, C. Wang, Y. Yang, X. Wang, M. Zhu, B.S. Hsiao, Dual-Biomimetic Superhydrophobic Electrospun Polystyrene Nanofibrous Membranes for Membrane Distillation, ACS Appl. Mater. Interfaces. 6 (2014) 2423–2430. doi:10.1021/am4048128.

[17] F. Liu, N.A. Hashim, Y. Liu, M.R.M. Abed, K. Li, Progress in the production and modification of PVDF membranes, J. Memb. Sci. 375 (2011) 1–27. doi:10.1016/J.MEMSCI.2011.03.014.

[18] E.-J. Lee, A.K. An, P. Hadi, S. Lee, Y.C. Woo, H.K. Shon, Advanced multi-nozzle electrospun functionalized titanium dioxide/polyvinylidene fluoride-co-hexafluoropropylene (TiO2/PVDF-HFP) composite membranes for direct contact membrane distillation, J. Memb. Sci. 524 (2017) 712–720. doi:10.1016/J.MEMSCI.2016.11.069.

[19] Y. Liao, C.-H. Loh, R. Wang, A.G. Fane, Electrospun Superhydrophobic Membranes with Unique Structures for Membrane Distillation, ACS Appl. Mater. Interfaces. 6 (2014) 16035–16048. doi:10.1021/am503968n.

[20] L.D. Tijing, Y.C. Woo, W.-G. Shim, T. He, J.-S. Choi, S.-H. Kim, H.K. Shon, Superhydrophobic nanofiber membrane containing carbon nanotubes for high-performance direct contact membrane distillation, J. Memb. Sci. 502 (2016) 158–170. doi:10.1016/J.MEMSCI.2015.12.014.

[21] H. Cho, J. Jeong, W. Kim, D. Choi, S. Lee, W. Hwang, Conformable superoleophobic surfaces with multi-scale structures on polymer substrates, J. Mater. Chem. A. (2016). doi:10.1039/C6TA02159J.

[22] C. Boo, J. Lee, M. Elimelech, Omniphobic Polyvinylidene Fluoride (PVDF) Membrane for Desalination of Shale Gas Produced Water by Membrane Distillation, Environ. Sci. Technol. 50 (2016) 12275–12282. doi:10.1021/acs.est.6b03882.

[23] F. Li, Z. Wang, S. Huang, Y. Pan, X. Zhao, Flexible, Durable, and Unconditioned Superoleophobic/Superhydrophilic Surfaces for Controllable Transport and Oil-Water Separation, Adv. Funct. Mater. 28 (2018) 1706867. doi:10.1002/adfm.201706867.

[24] X. Yue, J. Li, T. Zhang, F. Qiu, D. Yang, M. Xue, In situ one-step fabrication of durable superhydrophobic-superoleophilic cellulose/LDH membrane with hierarchical structure for efficiency oil/water separation, Chem. Eng. J. 328 (2017) 117–123. doi:10.1016/J.CEJ.2017.07.026.

[25] E.-J. Lee, B.J. Deka, J. Guo, Y.C. Woo, H.K. Shon, A.K. An, Engineering the Re-Entrant Hierarchy and Surface Energy of PDMS-PVDF Membrane for Membrane Distillation Using a Facile and Benign Microsphere Coating, Environ. Sci. Technol. 51 (2017) 10117–10126. doi:10.1021/acs.est.7b01108.

[26] H. Liu, J. Huang, Z. Chen, G. Chen, K.-Q. Zhang, S.S. Al-Deyab, Y. Lai, Robust translucent superhydrophobic PDMS/PMMA film by facile one-step spray for self-cleaning and efficient emulsion separation, Chem. Eng. J. 330 (2017) 26–35. doi:10.1016/J.CEJ.2017.07.114.

[27] Y. Chul Woo, Y. Chen, L.D. Tijing, S. Phuntsho, T. He, J.-S. Choi, S.-H. Kim, H. Kyong Shon, CF4 plasma-modified omniphobic electrospun nanofiber membrane for produced water brine treatment by membrane distillation, J. Memb. Sci. 529 (2017) 234–242. doi:10.1016/J.MEMSCI.2017.01.063.

[28] L. Li, B. Li, J. Dong, J. Zhang, Roles of silanes and silicones in forming superhydrophobic and superoleophobic materials, J. Mater. Chem. A. 4 (2016) 13677–13725. doi:10.1039/C6TA05441B.

[29] S. Gao, X. Dong, J. Huang, S. Li, Y. Li, Z. Chen, Y. Lai, Rational construction of highly transparent superhydrophobic coatings based on a non-particle, fluorine-free and water-rich system for versatile oil-water separation, Chem. Eng. J. 333 (2018) 621–629. doi:10.1016/J.CEJ.2017.10.006.

[30] W. Qing, X. Shi, W. Zhang, J. Wang, Y. Wu, P. Wang, C.Y. Tang, Solvent-Thermal Induced Roughening: a Novel and Versatile Method to Prepare Superhydrophobic Membranes, J. Memb. Sci. (2018). doi:10.1016/J.MEMSCI.2018.07.035.

[31] I.S. Chronakis, Novel nanocomposites and nanoceramics based on polymer nanofibers using electrospinning process—A review, J. Mater. Process. Technol. 167 (2005) 283–293. doi:10.1016/J.JMATPROTEC.2005.06.053.

[32] A. Chapiro, Z. Mankowski, N. Schmitt, Unusual swelling behavior of films of polyvinyl- and polyvinylidene/fluorides in various solvents, J. Polym. Sci. Polym. Chem. Ed. 20 (1982) 1791–1796. doi:10.1002/pol.1982.170200712.

[33] A.F.M. Barton, CRC handbook of polymer-liquid interaction parameters and solubility parameters, CRC Press, 1990. https://books.google.com.hk/books?hl=en&lr=&id=vzM-tMSwRZoC&oi=fnd&pg=PA3&dq=Handbook+of+Polymer–Liquid+Interaction+Parameters+and+Solubility+Parameters,&ots=y3ohb5g2or&sig=RAghItqfqIST0afTFR9gDWSV5Ww&redir_esc=y#v=onepage&q=Handbook of Polymer–Liquid Interaction Parameters and Solubility Parameters%2C&f=false (accessed December 13, 2017).

[34] D. Yang, D.J. Devlin, R.S. Barbero, Effect of hollow fiber morphology and compatibility on propane/propylene separation, J. Memb. Sci. 304 (2007) 88–101. doi:10.1016/J.MEMSCI.2007.07.005.

[35] C.M. Hansen, Hansen solubility parameters : a user's handbook., CRC Press, 2007. https://books.google.com.hk/books?hl=en&lr=&id=gprF31cvT2oC&oi=fnd&pg=PP1&dq=%22hansen+solubility+parameter%22&ots=KhbaGESi9g&sig=CjgtzEj4uXpwoAs94f6UmUoFGRo&redir_esc=y#v=onepage&q=%22hansen solubility parameter%22&f=false (accessed December 20, 2017).

[36] A. Bottino, G. Camera-Roda, G. Capannelli, S. Munari, The formation of microporous polyvinylidene difluoride membranes by phase separation, J. Memb. Sci. 57 (1991) 1–20. http://www.sciencedirect.com/science/article/pii/S037673880081159X (accessed December 12, 2013).

[37] J. Yuan, X. Liu, O. Akbulut, J. Hu, S.L. Suib, J. Kong, F. Stellacci, Superwetting nanowire membranes for selective absorption., Nat. Nanotechnol. 3 (2008) 332–6. doi:10.1038/nnano.2008.136.

[38] S. Munirasu, F. Banat, A.A. Durrani, M.A. Haija, Intrinsically superhydrophobic PVDF membrane by phase inversion for membrane distillation, Desalination. 417 (2017) 77–86. doi:10.1016/J.DESAL.2017.05.019.

[39] S. Al-Gharabli, W. Kujawski, H.A. Arafat, J. Kujawa, Tunable separation via chemical functionalization of polyvinylidenefluoride membranes using piranha reagent, J. Memb. Sci. 541 (2017) 567–579. doi:10.1016/J.MEMSCI.2017.07.047.

[40] H. Deng, Y. Dong, C. Zhang, Y. Xie, C. Zhang, J. Lin, An instant responsive polymer driven by anisotropy of crystal phases, Mater. Horizons. (2018). doi:10.1039/C7MH00854F.

[41] L. Li, M. Zhang, M. Rong, W. Ruan, Studies on the transformation process of PVDF from α to β phase by stretching, RSC Adv. 4 (2014) 3938–3943. doi:10.1039/C3RA45134H.

[42] C. Wan, C.R. Bowen, Multiscale-structuring of polyvinylidene fluoride for energy harvesting: the impact of molecular-, micro- and macro-structure, J. Mater. Chem. A. 5 (2017) 3091–3128. doi:10.1039/C6TA09590A.

[43] T. Xiao, P. Wang, X. Yang, X. Cai, J. Lu, Fabrication and characterization of novel asymmetric polyvinylidene fluoride (PVDF) membranes by the nonsolvent thermally induced phase separation (NTIPS) method for membrane distillation applications, J. Memb. Sci. 489 (2015) 160–174. doi:10.1016/J.MEMSCI.2015.03.081.

[44] M. Li, H.J. Wondergem, M.-J. Spijkman, K. Asadi, I. Katsouras, P.W.M. Blom, D.M. de Leeuw, Revisiting the δ-phase of poly(vinylidene fluoride) for solution-processed ferroelectric thin films, Nat. Mater. 12 (2013) 433–438. doi:10.1038/nmat3577.

[45] S.S. Latthe, P. Sudhagar, A. Devadoss, A.M. Kumar, S. Liu, C. Terashima, K. Nakata, A. Fujishima, A mechanically bendable superhydrophobic steel surface with self-cleaning and corrosion-resistant properties, J. Mater. Chem. A. 3 (2015) 14263–14271. doi:10.1039/C5TA02604K.

[46] S. Srinivasan, V.K. Praveen, R. Philip, A. Ajayaghosh, Bioinspired Superhydrophobic Coatings of Carbon Nanotubes and Linear π Systems Based on the "Bottom - up" Self - Assembly Approach, Angew. Chemie. 120 (2008) 5834–5838. doi:10.1002/ange.200802097.

[47] *,† Lin Feng, § Yanan Zhang, ‖ Jinming Xi, ‡ Ying Zhu, ‡ Nü Wang, ‡ and Fan Xia, ‡ Lei Jiang*, Petal Effect: A Superhydrophobic State with High Adhesive Force, (2008). doi:10.1021/LA703821H.

[48] A. Marmur, The Lotus Effect: Superhydrophobicity and Metastability, Langmuir. 20 (2004) 3517–3519. doi:10.1021/la036369u.

[49] L.D. Tijing, Y.C. Woo, W.-G. Shim, T. He, J.-S. Choi, S.-H. Kim, H.K. Shon, Superhydrophobic nanofiber membrane containing carbon nanotubes for high-performance direct contact membrane distillation, J. Memb. Sci. 502 (2016) 158–170. doi:10.1016/j.memsci.2015.12.014.